Supplement of Biogeosciences, 22, 863–957, 2025
https://doi.org/10.5194/bg-22-863-2025-supplement

Biogeosciences Open Access EGU

Supplement of

Reviews and syntheses: Review of proxies for low-oxygen paleoceanographic reconstructions

Babette A.A. Hoogakker et al.

Correspondence to: Babette A.A. Hoogakker (b.hoogakker@hw.ac.uk) and Catherine Davis (cdavis24@ncsu.edu)

Supplementary information

Section Introduction 'Challenges of seawater oxygen simulations'

One of the main challenges in modelling concentrations of marine oxygen is the representation of ocean physics, which in some regions crucially depends on small-scale processes. A realistic representation of OMZs (Busecke et al., 2019; Montes et al., 2014), and deep-water formation (Heuzé, 2021) requires high(er)-resolution ocean models. Eddy-resolving ocean models are best suited to represent these regions and water masses, but these high-resolution models are computationally very expensive. They cannot be integrated long enough for the simulated ocean and its tracers to reach equilibrium. Seawater oxygen content in the deep ocean is a tracer that needs especially long equilibrium times, requiring simulations of thousands of model years. Another challenge is the representation of biogeochemical processes in models (Fennel et al., 2022). Half of the CMIP6 coupled climate and Earth System models do not include any representation of marine biogeochemistry (IPCC, 2021: Annex II). If they do, the mathematical representations of marine ecosystems and biogeochemistry are quite simple. These ecosystem models are also under-constrained and tuned to reproduce present day observations. Any existing physical model biases will, thus, impact the biogeochemical parameters and lead to biogeochemical (including oxygenation) biases (Duteil et al, 2012). In addition, these models are missing important processes. For example, most climate models include NPZD (nutrient, phytoplankton, zooplankton, detritus) models with only one single phytoplankton functional type representing the biodiversity of the whole planet. Only a few models consider several nutrients and/or several phytoplankton functional types that can then compete against each other for nutrients and light. These more complex models are able to simulate ecosystem shifts due to changes in climate and nutrient availability and resolve species competition at regional scale. Shifts in predominant plankton types may be important as they can result in changes in the local abundance, size, sinking speed and quality of sinking organic particles, and therefore remineralisation depth and oxygen levels. But more complex models have even more tuneable parameters and are therefore even more under-constrained than the simple NPZD models (Andersen, 2005). Finally, feedbacks involving sediment/ocean fluxes that can impact biogeochemistry, biology, and therefore oxygen concentrations, such as the release of phosphorus and iron from anoxic sediments (Niemeyer et al., 2017), are generally not included in current models.

Section 6.3 'Biomarkers'

Table S1 Compilation of biomarker proxies indicative of oxygen-limited conditions.

proxy (compound or compound ratio)	source organism(s)	metabolism	environmental implication	reference
nitrogen cycling				
bacteriohopanetetrol-x (BHT-x)	'Ca. Scalindua profunda'	anammox	hypoxia/anoxia, O_2 <20µmol	Schwartz-Narbonne et al., 2020
BHT-x/[BHT+BHT-x]) ≥ 0.2	'Ca. Scalindua profunda' / bacteria	anammox	O_2 <50 µmol	van Kemenade et al. (2022)
3-Me-bacteriohopanehexol	Ca. Methylomirabilis oxyfera	n-damo	anoxia	Kool et al., 2014
3Me-bacteriohopanepentol	Ca. Methylomirabilis oxyfera	n-damo	anoxia	Kool et al., 2014
22,29,30-trisnorhopan-21-ol	Ca. Methylomirabilis oxyfera	n-damo	anoxia	Smit et al., 2019
3Me-22,29,30-trisnorhopan-21-ol	Ca. Methylomirabilis oxyfera	n-damo	anoxia	Smit et al., 2019

3Me-22,29,30-trisnorhopan-21-one	Ca. Methylomirabilis oxyfera	n-damo	anoxia	Smit et al., 2019
sulfur cycling				
isorenieratene	green sulfur bacteria (Chlorobiaceae)	sulfide oxidation	photic zone euxinia	Summons and Powell (1987), French et al. (2015)
isorenieratane	green sulfur bacteria (Chlorobiaceae)	sulfide oxidation	photic zone euxinia	Summons and Powell (1987), French et al. (2015)
2,3,6-trimethyl aryl isoprenoids			photic zone euxinia	Schwark and Frimmel (2004)
chlorobactene	green sulfur bacteria (Chlorobiaceae)	sulfide oxidation	photic zone euxinia	Schaeffer et al. (1997)
chlorobactane	green sulfur bacteria (Chlorobiaceae)	sulfide oxidation	photic zone euxinia	Schaeffer et al. (1997)
okenone	purple sulfur bacteria (Chromatiaceae)	sulfide oxidation	photic zone euxinia	Brocks and Schaeffer (2008)
okenane	purple sulfur bacteria (Chromatiaceae)	sulfide oxidation	photic zone euxinia	Brocks and Schaeffer (2008)
bacteriochlorophyll-c,d,e	green sulfur bacteria	sulfide oxidation	photic zone euxinia	Grice et al. (1996)
3-isobutyl-4-methylmaleimide	green sulfur bacteria	sulfide oxidation	photic zone euxinia	Grice et al. (1996), Naeher et al. (2013)
monoalkyl glycerol ethers (MAGEs)	sulfate reducing bacteria	sulfate reduction	anoxia	Bradley et al. (2009)
dialkyl glycerol ethers (DAGEs)	sulfate reducing bacteria	sulfate reduction	anoxia	Bradley et al. (2009)
^{13}C-depleted C16:1ω5 cy-C17:0ω5,6 C17:1ω6 alkanoic acids	sulfate reducing bacteria	sulfate reduction	anoxia	Niemann and Elvert (2008)
carbon cycling				
GDGT-0/crenarchaeol >2	methanogenic Euryarchaeota	methanogenesis	anoxia	Blaga et al. (2009)

coenzyme F430	methanogenic Euryarchaeota	methanogenesis	anoxia	Kaneko et al. (2021)
crocetane (tetramethylhexadecane)	ANME archaea	anaerobic methanotrophy	anoxia	Elvert et al. (1999)
(unsaturated) PMI (pentamethylicosane)	ANME archaea	anaerobic methanotrophy	anoxia	Elvert et al. (1999)
hydroxyarchaeol	ANME archaea	anaerobic methanotrophy	anoxia	Hinrichs et al. (2000; 2003)
aminopentol, methylcarbamate-bacteriohopanepentol	Type I methanotrophic bacteria	aerobic methanotrophy	methane-rich environment	Rush et al. (2016)
methylene-ubiquinone $MQ_{8:7}$	Type I methanotrophic bacteria	aerobic methanotrophy	methane-rich environment	Nowicka and Kruk (2010)
methylcarbamate-bacteriohopanetetrol	Type II methanotrophic bacteria	aerobic methanotrophy	methane-rich environment	Rush et al. (2016)
redox products				
pristane/phytane <1	chlorophyll-producing organisms	abiotic	anoxia	Peters et al. (2005)
pyropheophytin	chlorophyll-producing organisms	abiotic	anoxia	Szymczak-Żyla et al. (2008)
steryl chlorin esters	chlorophyll-producing organisms	abiotic	anoxia	Szymczak-Żyla et al. (2008)
high homohopane index	bacteria	abiotic	anoxia	Peters et al. (2005)
orphan biomarkers (unknown source)				
high lycopane/C_{31} n-alkane	unknown	methanogenesis?	anoxia	Sinninghe Damsté et al. (2003)
OB-GDGTs	unknown bacteria	unknown	anoxia	Liu et al. (2014), Connock et al. (2022)

Section 11 'Benthic foraminifera carbon isotope offsets'

Table S2. Data used to put together Figure 14.

Reference	Location	Core name	Lat	Lon	Water Depth	d13C of DIC	GLODAP oxygen (umol/kg)	WOA18 oxygen (umol/kg)	WOCE oxygen (umol/kg)	Average oxygen (umol/kg)	Average oxygen (umol/kg) 1stdev	Cib d18O	Cib d13C	Cib Species	Globobulimina d18O	Globobulimina d13C	Globobulimina species	Dd13C	Dd13C 1stdev	
Schmiedl and Mackensen, 2006	'Arabian'	'GeoB3004'	14.6	52.9	1803	-0.13	81.34	83.46	81.78	82.19	1.12	NaN	-0.05	'C. wuellerstorfi'	NaN	-1.01	G. affinis'	0.96	0.23	Figure 14
Costa et al., 2023	'Atlantic'	'KNR197-3-24MC'	7.59	-53.92	383	0.72	118.20	123.74	117.24	119.73	3.51	1.91	0.82	'C. pachyderma'	2.62	-0.05	'G. affinis'	0.87	0.32	Figure 14
Costa et al., 2023	'Atlantic'	'KNR197-3-2MC'	7.66	-53.82	556	0.68	118.93	124.56	118.18	120.55	3.49	1.92	0.39	'C. pachyderma'	2.31	-0.73	'G. affinis'	1.12	0.32	Figure 14
Costa et al., 2023	'Atlantic'	'KNR197-3-26MC'	7.72	-53.78	704	0.7	128.42	130.56	127.78	128.92	1.45	1.88	0.55	'C. pachyderma'	2.68	-0.69	'G. affinis'	1.24	0.32	Figure 14
Costa et al., 2023	'Atlantic'	'KNR197-3-28MC'	7.84	-53.67	962	0.71	150.26	150.96	149.33	150.18	0.81	2.34	0.56	'C. pachyderma'	3.15	-0.90	'G. affinis'	1.46	0.32	Figure 14
Costa et al., 2023	'Atlantic'	'KNR197-3-17MC'	7.44	-52.76	1029	0.77	154.20	159.59	152.41	155.40	3.74	2.49	0.89	'C. pachyderma'	2.74	-0.75	'G. affinis'	1.64	0.32	Figure 14
Costa et al., 2023	'Atlantic'	'KNR197-3-10MC'	7.94	-53.58	1107	0.83	173.72	172.10	171.92	172.58	0.99	2.44	0.80	'C. pachyderma'	3.09	-0.88	'G. affinis'	1.68	0.32	Figure 14
Costa et al., 2023	'Atlantic'	'KNR197-3-33MC'	8.25	-53.24	1275	0.98	200.91	200.04	196.64	199.20	2.26	2.47	1.02	'C. pachyderma'	3.26	-0.71	'G. affinis'	1.73	0.32	Figure 14
Thomas et al., 2022	'Atlantic'	'JC89-11'	37.86	9.34	628	0.84	188.19	186.16	197.23	190.53	5.89	NaN	1.05	'C. mundulus'	NaN	-0.79	'G. affinis'	1.84	0.14	Figure 14
Thomas et al., 2022	'Atlantic'	'JC89-10'	37.84	9.51	1127	0.84	186.65	188.27	188.95	187.96	1.18	NaN	0.56	'C. mundulus'	NaN	-1.09	'G. affinis'	1.65	0.14	Figure 14
Thomas et al., 2022	'Atlantic'	'JC89-13'	37.94	9.59	1448	0.98	201.47	191.71	141.19	178.13	32.35	NaN	0.89	'C. mundulus'	NaN	-1.40	'G. affinis'	2.29	0.14	Figure 14
Thomas et al., 2022	'Atlantic'	'JC89-09'	37.83	9.82	2323	0.93	220.34	191.26	172.46	194.69	24.12	NaN	0.29	'C. mundulus'	NaN	-3.45	'G. affinis'	3.74	0.14	Figure 14
Thomas et al., 2022	'Atlantic'	'JC89-08'	37.78	10.05	2619	0.87	216.18	193.14	170.60	193.31	22.79	NaN	0.56	'C. mundulus'	NaN	-2.69	'G. affinis'	3.25	0.14	Figure 14
Thomas et al., 2022	'Atlantic'	'JC89-06'	37.56	10.14	2645	0.84	216.46	193.32	172.72	194.17	21.88	NaN	0.49	'C. mundulus'	NaN	-2.23	'G. affinis'	2.72	0.14	Figure 14
Mackensen and Licari, 2004	'Atlantic'	'GeoB3708'	-21.1	11.8	1283	0.73	185.99	181.11	179.98	182.36	3.20	NaN	0.48	'C. wuellerstorfi'	NaN	-1.27	'G. pacifica'	1.75	0.23	Figure 14 & 16
Mackensen and Licari, 2004	'Atlantic'	'GeoB3706'	-22.7	12.6	1313	0.73	187.38	183.82	181.19	184.13	3.11	NaN	0.64	'C. wuellerstorfi'	NaN	-1.15	'G. pacifica'	1.79	0.23	Figure 14 & 16
Thomas et al., 2022	'Atlantic'	'JC89-13'	37.94	9.59	1448	0.98	201.47	191.71	141.19	178.13	32.35	NaN	1.14	'C. wuellerstorfi'	NaN	-1.40	'G. affinis'	2.54	0.23	Figure 14 & 16
McKay et al., 2016	'Atlantic'	'GeoB3606-1'	-25.47	13.08	1785	0.83	213.34	214.25	211.19	212.93	1.57	2.64	0.50	'C. wuellerstorfi'	3.43	-1.40	'G. turgida'	1.90	0.23	Figure 14 & 16
Mackensen and Licari, 2004	'Atlantic'	'GeoB3725'	-23.3	12.4	1980	0.93	227.00	223.27	221.57	223.95	2.77	NaN	0.60	'C. wuellerstorfi'	NaN	-1.30	'G. pacifica'	1.90	0.23	Figure 14 & 16
Costa et al., 2023	'Atlantic'	'KNR197-3-41MC'	8.38	-53.05	2052	1.04	255.86	256.28	254.56	255.56	0.90	2.53	1.14	'C. wuellerstorfi'	3.64	-1.46	'G. affinis'	2.60	0.23	Figure 14 & 16
Hoogakker et al., 2015	'Atlantic'	'RAPID 11 7B/RAPID	62.3	-17.15	2126	0.98	279.07	276.96	280.55	278.86	1.80	2.74	1.29	'C. wuellerstorfi'	3.58	-1.84	'G. pacifica'	3.13	0.23	Figure 14 & 16
Thomas et al., 2022	'Atlantic'	'JC89-09'	37.83	9.82	2323	0.93	220.34	191.26	172.46	194.69	24.12	NaN	0.76	'C. wuellerstorfi'	NaN	-3.45	'G. affinis'	4.21	0.23	Figure 14 & 16
Costa et al., 2023	'Atlantic'	'KNR197-3-37MC'	8.43	-52.79	2440	1.09	256.98	257.72	256.37	257.02	0.68	2.64	1.39	'C. wuellerstorfi'	3.82	-1.51	'G. affinis'	2.90	0.23	Figure 14 & 16
Thomas et al., 2022	'Atlantic'	'JC89-08'	37.78	10.05	2619	0.87	216.18	193.14	170.60	193.31	22.79	NaN	1.09	'C. wuellerstorfi'	NaN	-2.69	'G. affinis'	3.78	0.23	Figure 14 & 16
Thomas et al., 2022	'Atlantic'	'JC89-06'	37.56	10.14	2645	0.84	216.46	193.32	172.72	194.17	21.88	NaN	1.05	'C. wuellerstorfi'	NaN	-2.23	'G. affinis'	3.28	0.23	Figure 14 & 16
Costa et al., 2023	'Atlantic'	'KNR197-3-35MC'	8.47	-52.79	3328	1.1	258.94	258.55	258.67	258.72	0.20	2.73	1.17	'C. wuellerstorfi'	3.93	-1.66	'G. affinis'	2.83	0.23	Figure 14 & 16
Lu et al., 2022	'Indian'	'TN041-8PG/8JPC'	17.8	57.5	761	-0.1	7.44	10.75	7.18	8.46	1.99	1.67	0.41	unidentified'	1.79	-0.22	'G. affinis'	0.63	0.51	Figure 14
Hoogakker et al., 2015	'Pacific'	'ODP 1242'	7.86	-83.61	1364	-0.17	97.69	87.58	91.36	92.21	5.11	2.57	0.36	'C. wuellerstorfi'	3.65	-0.72	'mixed'	1.08	0.23	Figure 14 & 16
Hoogakker et al., 2015	'Pacific'	'TR163-25'	-1.65	-88.45	2650	0.04	117.74	123.29	118.64	119.89	2.98	2.80	0.14	'C. wuellerstorfi'	3.51	-1.55	G.affinis'	1.69	0.23	Figure 14 & 16
Umling and Thunel, 2018	'Pacific'	'TR163-23'	0.41	-92.16	2730	-0.02	117.73	124.30	118.23	120.09	3.66	2.66	0.16	'C. wuellerstorfi'	3.49	-1.62	'G. affinis'	1.78	0.23	Figure 14 & 16
Jacobel et al., 2020	'Pacific'	'ODP 1240'	0.02	-86.46	2921	0.01	122.22	125.09	125.08	124.13	1.65	3.33	0.22	'C. wuellerstorfi'	3.49	-1.94	'G. affinis'	2.15	0.23	Figure 14 & 16
Jacobel et al., 2020	'Pacific'	'ODP 846'	-3.09	-90.82	3295	0.08	138.56	135.42	139.93	137.97	2.31	2.80	-0.14	'C. wuellerstorfi'	3.66	-1.75	'G. affinis'	1.61	0.23	Figure 14 & 16

Below follows a morphological description of the benthic foraminifera used to reconstruct bottom water oxygen concentrations through $\Delta\delta^{13}C$:

The most commonly used foraminifer is *Cibicidoides wuellerstorfi* (Schwager), 1866. Following the description of Loeblich and Tappan (1988) and Holbourn et al. (2013), C. wuellerstorfi has typically a very low trochospiral, compressed and planoconvex test, eight to twelve chambers visible in the final whorl that curve back at the periphery, with an (partially) evolute spiral (umbilical) side and a keeled periphery. About ten elongated and curved chambers in the final whorl are separated by strongly curved sutures that are slightly depressed in the final chambers on the spiral side. The spiral (umbilical) side is coarsely (finely) perforated and the interiomarginal aperture of *C. wuellerstorfi* features a narrow lip. One particular sensu lato morphotype of C. wuellerstorfi has been described previously and is commonly found in southern high-latitude marine environments (Gottschalk et al., 2016; Rae et al., 2011). While it shares many characteristics with *C. wuellerstorfi*, in particular the trochospiral, plano-convex test and perforation features, it has often only seven to nine chambers in the final whorl that are wider and more inflated than in the sensu stricto morphotype of *C. wuellerstorfi*. The test of the sensu lato morphotype shows intercameral sutures that are not as strongly curved towards the periphery as seen in the sensu stricto morphotype and appears duller in reflectance.

When *C. wuellerstorfi* is absent in the sedimentary record, other foraminiferal species thought to approximate an epifaunal habitat like *Cibicides kullenbergi* (Parker), 1953 (synonymously used with *Cibicidoides mundulus* (Brady, Parker, and Jones), 1888) have also been used to reconstruct bottom water oxygen levels using the $\Delta\delta^{13}C$ proxy [e.g., Gottschalk et al., 2016a, 2020; Bunzel et al., 2017; Lu et al., 2022]. While *C. kullenbergi* specimens are similar to *C. wuellerstorfi* (i.e., showing a trochospiral test, ten to eleven chambers in the final whorl, similar perforation intensities, aperture with a thin lip, and arched sutures on the spiral side), it is biconvex in cross-section. The length to width ratio of chambers in *C. kullenbergi* is much smaller and intercameral sutures are less curved than in *C. wuellerstorfi*. However, intergrades between *C. kullenbergi* sensu stricto and *C. wuellerstorfi* sensu stricto are common, leading not only to specimen with similarity to *C. wuellerstorfi* (*C. wuellerstorfi* sensu lato) but also to specimen with resemblance to *C. kullenbergi* (C. kullenbergi sensu lato). *C. kullenbergi* sensu lato tends to show a plano-convex test and a more sub-circular test compared to the biconvex, circular *C. kullenbergi* sensu stricto. In addition, the sutures of *C. kullenbergi* sensu lato are more strongly curved towards the periphery than those of *C. kullenbergi* sensu stricto, but not as strong as in *C. wuellerstorfi* sensu stricto or sensu lato. The chamber length-to-width ratio is also slightly greater in comparison to *C. kullenbergi* sensu stricto but not as high as seen in *C. wuellerstorfi* sensu stricto or sensu lato.

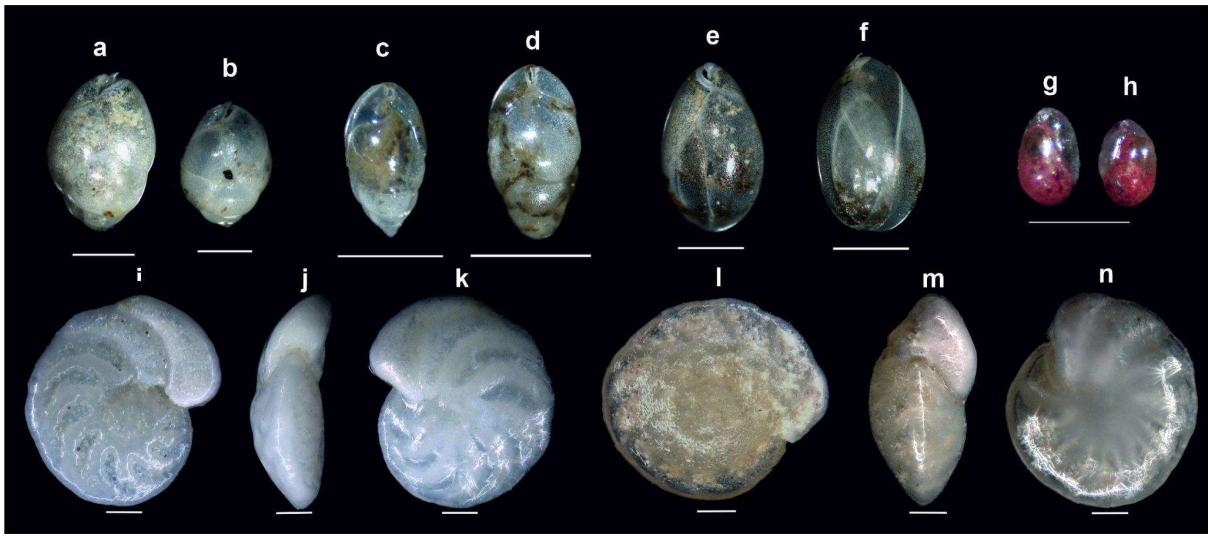

Figure S1. Overview of *Globobulimina* and *Cibicidoides/Cibicides* species that form the backbone of the $\Delta\delta^{13}C$ proxy. a, b) Lateral view of *Globobulimina auriculata* (a: ODP1014D 1H 4W, 97-99 cm; b: ODP1014D 1H 5W, 66-68 cm; scale = 1000 µm), c) lateral view of *Globobulimina affinis* (morphotype 1; ODP1014D 1H 5W, 7-9 cm; scale = 1000 µm), d) lateral view of *G. affinis* (morphotype 2; ODP1014D 1H 5W, 7-9 cm; scale = 1000 µm), e, f) lateral view of *Globobulimina pacifica* (ODP1014D 1H 4W, 129-131 cm; scale = 1000 µm), g, h) lateral view of *Globobulimina turgida* (GeoB15022-2, 1-2 cm; scale = 350 µm), i, j, k) spiral, lateral and umbilical view of *Cibicidoides wuellerstorfi* sensu stricto (TNO57-6GC 44-46 cm; scale = 100 µm), and l, m, n) spiral, lateral and umbilical view of *Cibicides kullenbergi* sensu stricto (MD97-2100, 20-21 cm; scale = 100 µm).

Figure 3 below shows the relationship between the benthic foraminiferal carbon isotope gradient and bottom water oxygen, including species that sometimes may change their depth habitat between epi- and infaunal (see section 6.8.5 for more details).

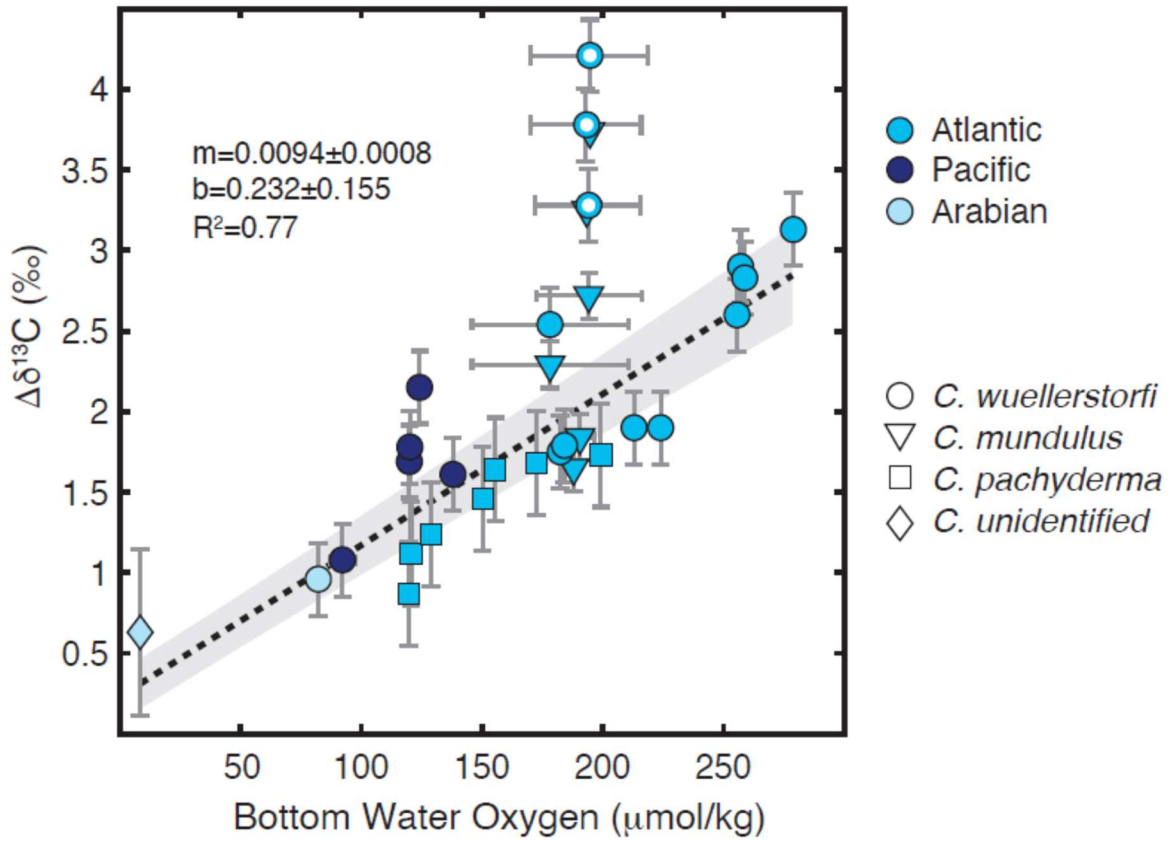

Figure S2: Extended Figure 14, showing $\Delta\delta^{13}C$ of other *Cibicidoides species* versus *Globobulimina* (spp.) and bottom water oxygen. White circles represent outliers that were excluded from the regression. Bottom water oxygen concentrations shown are average between GLODAP, WOA18 and WOCE data (see Table S2).

Section 13 'Data management and transparency'

Table S3. Examples of file structure and data organization; PANGAEA and other repositories provide extensive details about which meta data is required with core submission:

File type	Necessary information that need to content and examples	name of the file

Sample location	Site name, ocean basin or sea, site name, latitude and longitude, water depth DOI code of the original publication	sitename_metadata.csv (e.g. GeoB15007-1_metadata.csv)
Sample details	Site name, depth information (details of conversions to MBSF or MCD in the case of ODP cores, unique sample number from core repository.	sitename_depth.csv
Age model	Site name (use the original name used in the expedition) (e.g. GeoB15007-1; 1014) Sample depth (m), dating technique (AMS dates, d18O stratigraphy, 210-Pb, other), age.	sitename_ageraw.csv
Foraminifera Assemblages	Site name, sample label, sample depth (m), sample size, splits and fraction, staining if applicable, foraminifera taxa, counts, example images DOI: publications	site_forams_assemblages.csv

Examples of working groups that are curating specific proxy data bases and links to websites.

FORCIS (Foraminifera response to Climatic Stress, currently active) are evaluating the biodiversity changes of calcifying zooplankton in response to multiple stressors (https://forcis.cerege.fr/). NICOPP (Global ocean sediment nitrogen isotope data base, inactive) was a joint group between PAGES and IMAGES studying nitrogen isotope dynamics from sedimentary records in the Quaternary and modern times (http://pastglobalchanges.org/science/wg/former/nicopp/). MOSAIC (Modern Ocean Sediment Archive and Inventory of Carbon, active) goal is to synthesize local, regional and global-scale of the content, source and fate of organic materials accumulating in contemporary marine sediments (http://mosaic.ethz.ch/). Finally, GLODAP (The Global Ocean Data Analysis Project) is an example of where physical and chemical hydrological data of water samples are stored (https://glodap.info/).

References:

Anderson, T.R.: Plankton functional type modelling: running before we can walk?, J. Plankton Res., 27, 1073-1081, https://doi.org/10.1093/plankt/fbi076, 2005.

Busecke, J., Resplandy, L., Dunne, J.P.: The Equatorial Undercurrent and the Oxygen Minimum Zone in the Pacific, Geophys. Res. Lett., 46, 6716-6725, https://doi.org/10.1029/2019GL082692, 2019.

Costa, K., Nielsen, S.G., Wang, Y., Lu, W., Hines, S.K.V., Jacobel, A.W., Oppo, D.W.: Marine sedimentary uranium to barium ratios as a potential quantitative proxy for Pleistocene bottom water oxygen concentrations, Geochimica et Cosmochimica Acta 343, 1-16, 2023.

Duteil, O., and Oschlies, A.: Sensitivity of simulated extent and future evolution of marine suboxia to mixing intensity: Sensitivity of suboxia to mixing intensity, Geophys. Res. Lett., 38, n/a-n/a, https://doi.org/10.1029/2011GL046877, 2011.

Duteil, O., Koeve, A., Oschlies, A., Aumont, O., Bianchi, D., Bopp, L., Galbraith, E., Mataer, R., Moore, J.K., Sarmiento, J.L., and Segschneider, J.: Preformed and regenerated phosphate in ocean general circulation

models: can right total concentrations be wrong?, Biogeosciences, 9, 1797-1807, https://doi.org/10.5194/bg-9-1797-2012, 2012.

Fennel, K., Mattern, J.P., Doney, S.C., Bopp, L., Moore, A.M., and Wang, B., Y, L.: Ocean biogeochemical modelling, Nat. Rev. Methods Primers 2, 76, https://doi.org/10.1038/s43586-022-00154-2, 2022.

Heuzé, C.: Antarctic Bottom Water and North Atlantic Deep Water in CMIP6 models, Ocean Sci., 17, 59-90, https://doi.org/10.5194/os-17-59-2021, 2021.

Hoogakker, B. A. A., Elderfield, H., Schmiedl, G., McCave, I. N., and Rickaby, R. E. M.: Glacial–interglacial changes in bottom-water oxygen content on the Portuguese margin, Nat. Geosci., 8, 40–43, https://doi.org/10.1038/ngeo2317, 2015.

Jacobel, A.W., Anderson, R.F., Jaccard, S.L., McManus, J.F., Pavia, F.J., and Winckler, G.: Deep Pacific storage of respired carbon during the last ice age: Perspectives from bottom water oxygen reconstructions, Quat. Sci. Rev., 230, 106065, https://doi.org/10.1016/j.quascirev.2019.106065, 2020.

Lu, W., Wang, Y., Oppo, D. W., Nielsen, S. G., and Costa, K. M.: Comparing paleo-oxygenation proxies (benthic foraminiferal surface porosity, I/Ca, authigenic uranium) on modern sediments and the glacial Arabian Sea, Geochim. Cosmochim. Ac., 331, pp.69-85, https://doi.org/10.1016/j.gca.2022.06.001, 2022.

Mackensen, A., Licari, L.: Carbon Isotopes of Live Benthic Foraminifera from the South Atlantic: Sensitivity to Bottom Water Carbonate Saturation State and Organic Matter Rain Rates, The South Atlantic in the Late Quaternary: Reconstruction of material budgets and current systems, 623-644, Springer Berlin Heidelberg, 2004.

McKay, C.L., Filipsson, H.L., Romero, O.E., Stuut, J.,-N.W., Björck, S.: The interplay between the surface and bottom water environment within the Benguela Upwelling System over the last 70 ka, Paleoceanography and Paleoclimatology 31, 266-285.

Montes, I., Dewitte, B,m Gutknecht, E., Paulmier, A., Dadou, I., Oschlies, A., Garcon, V., High-resolution modeling of the Eastern Tropical Pacific oxygen minimum zone: Sensitivity to the tropical oceanic circulation, J. Geophys. Res. Oceans, 119, 5515 –5532, doi:10.1002/2014JC009858, 2014.

Niemeyer, D., Kemena, T.P., Meissner, K.J., and Oschlies, A.: A model study of warming induced phosphorus-oxygen feedbacks in open-ocean oxygen minimum zones on millennial timescales, Earth Syst. Dynam., 8, 357-367, https://doi.org/10.5194/esd-8-357-2017, 2017.

Schmiedl, G., Mackensen, A.: Multispecies stable isotopes of benthic foraminifers reveal past changes of organic matter decomposition and deepwater oxygenation in the Arabian Sea, Paleoceanography and Paleoclimatology 21, PA4213, doi:10.1029/2006PA001284, 2006.

Thomas, N.C., Bradbury, H.J., Hodell, D.A.: Changes in North Atlantic deep-water oxygenation across the Middle Pleistocene Transition, Science 377, 654-659, 2022.

Umling, N. E., and Thunell, R. C.: Mid-depth respired carbon storage and oxygenation of the eastern equatorial Pacific over the last 25,000 years, Quaternary Sci. Rev., 189, 43-56, https://doi.org/10.1016/j.quascirev.2018.04.002, 2018.